CARBON letters

Note

Carbon Letters Vol. 27, 117-120 (2018)

Control of interlayer spacing of expanded graphite for improved hydrogen storage capacity

Hyo In Lee, Won Jong Kim, Young-Jung Heo, Yeong-Rae Son and Soo-Jin Park*

Department of Chemistry, Inha University, Incheon 22212, Korea

Article Info

Received 20 September 2017
Accepted 20 December 2017

***Corresponding Author**
E-mail: sjpark@inha.ac.kr
Tel: +82-32-876-7234

Open Access

DOI: http://dx.doi.org/10.5714/CL.2018.27.117

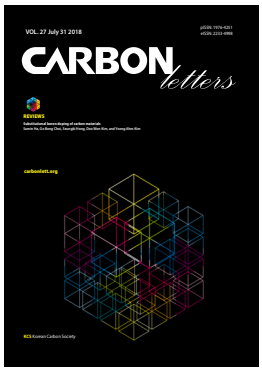

http://carbonlett.org

pISSN: 1976-4251
eISSN: 2233-4998

The World Meteorological Organization has officially announced that when the United States exits the Paris Climate Change Accord, it expects the average global temperature to rise by about 0.3°C this century [1-4]. Large amounts of carbon dioxide are being generated by the drastic increase in the use of fossil fuels due to global industrialization. Clean fuels that can replace them are the need of the hour [5-7]. One of the environmentally-friendly energy alternatives–hydrogen, which is readily available since more than 70% of the world is occupied by water–is attracting attention. Hydrogen burns in nitrogen and oxygen oxides, and harmful substances can be safely removed even at low temperatures. Hydrogen also has a higher energy content than petroleum products such as gasoline or diesel, and can be used as a source of energy in mobile phones, portable devices, and hydrogen vehicles [8-12].

The hydrogen storage methods developed so far include liquid hydrogen storage, gaseous hydrogen storage, hydrogen compression methods using metal hydrides, and adsorption methods. Liquid hydrogen storage or gaseous hydrogen storage methods are expensive; moreover, they pose a risk of explosion at room temperature. Hydrogen compression using metal hydrides is the easiest way to store hydrogen at a maximum of 20 bar; however, the approach has disadvantages in that the required equipment is heavy in weight and is expensive [9,13]. Methods of adsorption, namely, the solid hydrogen storage method, are potential solutions to overcome these problems. The adsorption method is highly advantageous in that the design is relatively simple and safe as compared to other methods [13-15].

A number of adsorbents can be used for solid hydrogen storage, including activated carbon, carbon nanotubes, silica, zeolite, and porous polymers [16-19]. In particular, carbon materials have excellent chemical stability, low environmental pollution, and high potential for industrial use as compared to other high strength, light weight, and high modulus materials; moreover, carbon can be easily obtained from nature [20-22]. Among carbon materials, graphite is composed of layers held together by van der Waals forces, which makes it easier to control the interlayer spacing using other chemical bonds, such as hydrogen bonds and covalent bonds. As a result, various atoms, molecules, and ions can be inserted in the graphite to produce a layered compound [23,24].

By controlling the interlayer spacing, it is possible to store more hydrogen by expanding the layers of graphite, and also store hydrogen at a much lower pressure and temperature (298 K) than conventional methods which require high pressure (100 bar) and temperature. This adsorption method provides advantages including stability and safety, and therefore wide applicability, and thus supports the use of hydrogen as a promising alternative source of energy [9,25].

In this study, expanded graphites (EGs) were prepared by a chemical method using H_2O_2 and $KMnO_4$. The effects of the surface area and interlayer spacing of EG on hydrogen storage at 298 K and 100 bar were studied.

For the synthesis of the EGs, graphite flakes (Sigma-Aldrich Co., USA), potassium permanganate ($KMnO_4$, ≥99.3%; OCI Co., Korea), sulfuric acid (H_2SO_4, 98%; Daejung Co., Korea), hydrogen peroxide (H_2O_2, ≥30%; OCI Co.), and thrice distilled water were used. All chemicals were used without further purification.

To prepare EG, first, 5 g of graphite flakes and 5 g of $KMnO_4$ were added into a 1000-mL beaker, after which 500 mL of 98% H_2SO_4 solution was added. After 10 min, 100 mL of H_2O_2 solution (30 wt%) was slowly added into the mixture. Samples were collected at 3, 6, 9,

and 12-h intervals, and the collected mixtures were sufficiently washed with thrice distilled water to adjust their pH to a nearly neutral value of 7. Subsequently the samples were dried at 80°C for 24 h. The prepared samples are henceforth denoted as EG-3, EG-6, EG-9, and EG-12, respectively.

To determine the structural characteristics and interlayer spacing of the EGs, X-ray diffraction (XRD; Bruker-AXS D2 PHASER, USA) using CuKα radiation and scanning electron microscopy (SEM; S-4300SE, Hitachi, Japan) was used. The hydrogen storage capacity was measured at 298 K and 100 bar using a BELSORP instrument (BELSORP-max; BEL Co., Ltd). For this, the samples were degassed at 473 K for 8 h to remove other impurities, cooled at room temperature, and then measured using ultra-high-purity hydrogen gas (99.9999%) until 298 K and 100 bar was reached. Finally, data were obtained using the adsorption-desorption isotherm of H_2 to determine the hydrogen storage capacity.

Fig. 1 shows a schematic of the hydrogen storage mechanism of EGs. The process of graphite expansion involves a massive

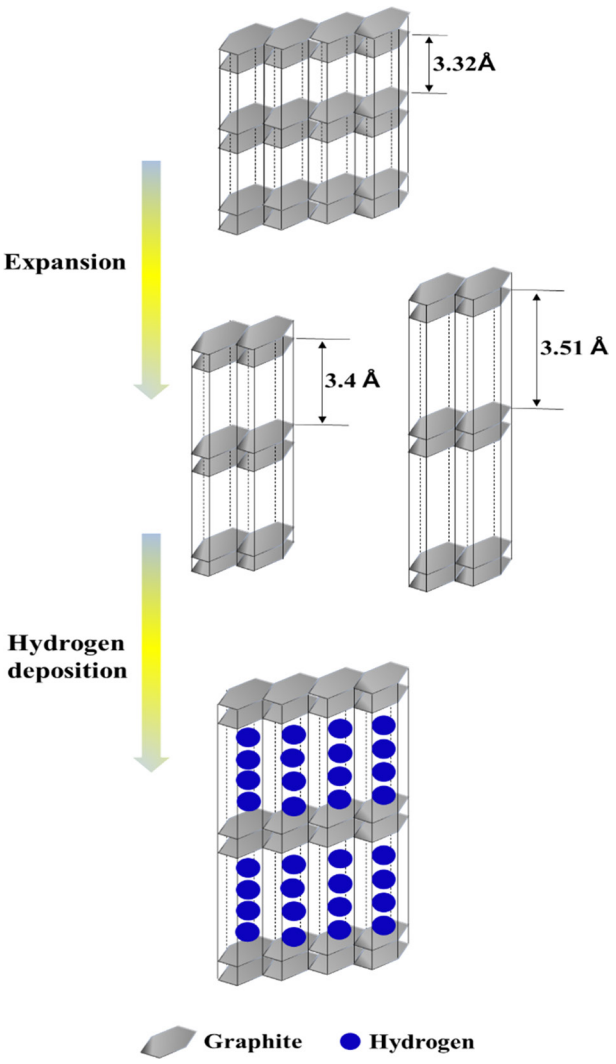

Fig. 1. Schematic of hydrogen storage mechanism in EGs.

increase in volume (~200 mL g^{-1}); as the crystalline structure of the graphite is destroyed, the expansion increases to ~70 to 100 times more than graphite flakes along the thickness or the direction of the c-axis [26,27]. Fig. 2 and Table 1 show the interlayer spacing of EGs with impregnation time in acid.

In Fig. 2a, the XRD patterns of the graphite flakes show two peaks: one at 26.6° for the (0 0 2) plane and the other at 54.7° for the (0 0 4) plane (JCPDS no. 41-1487). The patterns of all EG samples show similar peaks at 26.6°; however, these are of weak intensity, and the other peak at 54.7° almost disappears. These changes in XRD patterns imply a transformation in the graphitic structure, attributed to impregnation in $KMnO_4$, and is evidence of the change in interlayer spacing.

As the impregnation time increases, the peak intensity of the EG becomes lower because of a reduction in crystallinity attributed to expansion [28,29]. The peak positions are slightly shifted from the 26.6° with a '*d* spacing of 0.332 nm of graphite flakes, to 25.2° with a '*d* spacing of 0.351° of EG-6; the smaller angles indicate an increase in interlayer spacing. These results imply that EG-6 has the largest hydrogen storage capacity compared to other samples [30-33]. The peak at 10.8° with a '*d* spacing of 0.8 nm also indicate a reduction in crystallinity. The interlayer distance was calculated from the (002) peak of the XRD pattern using Bragg's law [34]:

$$n\lambda = 2d \sin \theta \quad (1)$$

where n is an integer, θ is the X-ray wavelength, d is the interlayer distance, and λ is the diffraction angle. The interlayer spacing gradually increased with time, reaching a maximum at

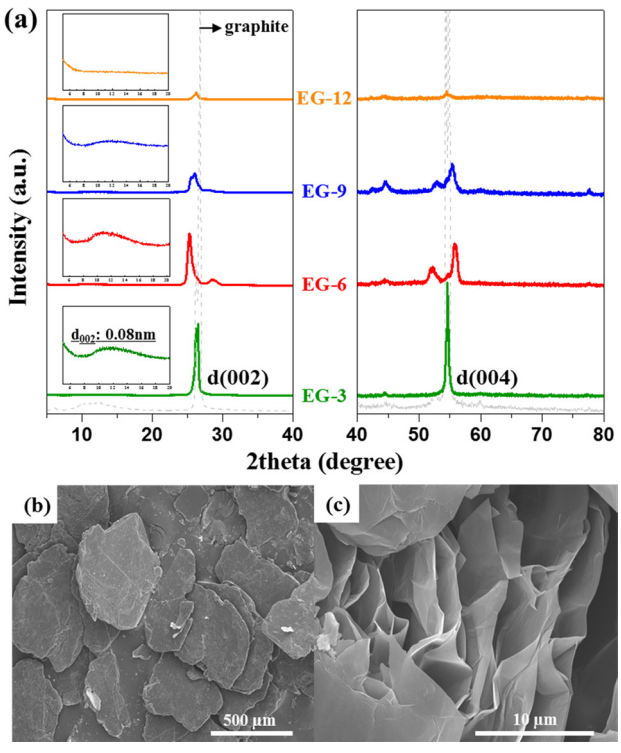

Fig. 2. (a) X-ray diffraction patterns of graphite and EGs, and SEM images of (b) conventional graphite flakes and (c) EG-6.

Table 1. Interlayer spacing between the graphite layers of the samples prepared

Composition	Gap length (Å)
Graphite flakes	3.32
EG-3	3.39
EG-6	3.51
EG-9	3.42
EG-12	3.39

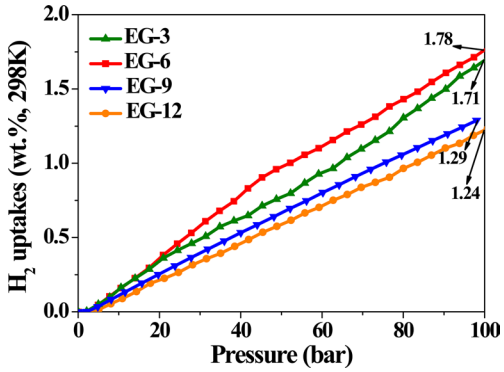

Fig. 3. Hydrogen storage capacities of EGs at 298 K.

6 h, and then gradually narrowed. This increase in the interlayer spacing of EG-6 as compared to conventional graphite flakes is also confirmed by the SEM images in Fig. 2b and c.

The hydrogen storage capacity in relation to the interlayer spacing of graphite flakes is shown in Fig. 3. The hydrogen storage capacity grew as the interlayer spacing increased with time, and gradually decreased after 6 h of impregnation time, with a reduction in interlayer spacing. Aga et al. [35] reported that as the interlayer spacing nears 6 Å, the hydrogen storage capacity increases. If the interlayer spacing is smaller, there is no place to accommodate hydrogen molecules. Therefore, since EG-6 had the highest interlayer spacing, it can be expected to have the highest hydrogen storage capacity, which tends to decrease with decreasing interlayer spacing [36-38].

In this study, under stable experimental conditions at room temperature and 100 bar, the effect of the interlayer spacing of EGs on hydrogen storage performance was investigated. The impregnation time for oxidation (3, 6, 9, and 12 h) was used as a variable. The interlayer spacing gradually increased and then decreased again with increasing impregnation time. The hydrogen storage capacity was the highest for sample EG-6; this result was also reflected in the interlayer spacing of the EGs, i.e., the hydrogen adsorption properties of the EGs greatly increased with the increase in interlayer spacing.

Conflict of Interest

No potential conflict of interest relevant to this article was reported.

Acknowledgements

This work was supported by an Inha University research grant, South Korea.

References

[1] Schlapbach L, Züttel A. Hydrogen-storage materials for mobile applications. Nature, **414**, 353 (2001). https://doi.org/10.1038/35104634.

[2] Slorach SA. The WHO/UNEP pilot project on assessment of human exposure to pollutants through biological monitoring. Environ Monit Assess, **2**, 33 (1982). https://doi.org/10.1007/bf00399153.

[3] Silanikove N, Koluman N. Impact of climate change on the dairy industry in temperate zones: predications on the overall negative impact and on the positive role of dairy goats in adaptation to earth warming. Small Ruminant Res, **123**, 27 (2015). https://doi.org/10.1016/j.smallrumres.2014.11.005.

[4] Woolsey TS. Two treaties of Paris. Am J Int Law, **13**, 81 (1919). https://doi.org/10.2307/2187976.

[5] Hsu CW. Constructing an evaluation model for hydrogen application pathways. Int J Hydrogen Energy, **38**, 15836 (2013). https://doi.org/10.1016/j.ijhydene.2013.05.100.

[6] Afgan NH, Carvalho MG. Sustainability assessment of hydrogen energy systems. Int J Hydrogen Energy, **29**, 1327 (2004). https://doi.org/10.1016/j.ijhydene.2004.01.005.

[7] Afgan NH, Veziroglu A, Carvalho MG. Multi-criteria evaluation of hydrogen system options. Int J Hydrogen Energy, **32**, 3183 (2007). https://doi.org/10.1016/j.ijhydene.2007.04.045.

[8] Dutta S. A review on production, storage of hydrogen and its utilization as an energy resource. J Ind Eng Chem, **20**, 1148 (2014). https://doi.org/10.1016/j.jiec.2013.07.037.

[9] Zhou L. Progress and problems in hydrogen storage methods. Renewable Sustainable Energy Rev, **9**, 395 (2005). https://doi.org/10.1016/j.rser.2004.05.005.

[10] Kaestner P, Michler T, Weidner H, Rie KT, Bräuer G. Plasma nitrided austenitic stainless steels for automotive hydrogen applications. Surf Coat Technol, **203**, 897 (2008). https://doi.org/10.1016/j.surfcoat.2008.08.024.

[11] Wind J, Späh R, Kaiser W, Böhm G. Metallic bipolar plates for PEM fuel cells. J Power Sources, **105**, 256 (2002). https://doi.org/10.1016/S0378-7753(01)00950-8.

[12] Murr LE, Staudhammer KP, Hecker SS. Effects of strain state and strain rate on deformation-induced transformation in 304 stainless steel: Part II. Microstructural study. Metall Mater Trans A, **13**, 627 (1982). https://doi.org/10.1007/BF02644428.

[13] Broom DP, Hirscher M. Irreproducibility in hydrogen storage material research. Energy Environ Sci, **9**, 3368 (2016). https://doi.org/10.1039/C6EE01435F.

[14] Ströbel R, Garche J, Moseley PT, Jörissen L, Wolf G. Hydrogen storage by carbon materials. J Power Sources, **159**, 781 (2006). https://doi.org/10.1016/j.jpowsour.2006.03.047.

[15] Klebanoff LE, Keller JO. 5 Years of hydrogen storage research in the U.S. DOE Metal Hydride Center of Excellence (MHCoE). Int J Hydrogen Energy, **38**, 4533 (2013). https://doi.org/10.1016/j.ijhydene.2013.01.051.

[16] Han YJ, Park SJ. Effect of nickel on hydrogen storage behaviors

of carbon aerogel hybrid. Carbon Lett, **16**, 281 (2015). https://doi.org/10.5714/CL.2015.16.4.281.

[17] Yildirim T, Ciraci S. Titanium-decorated carbon nanotubes as a potential high-capacity hydrogen storage medium. Phys Rev Lett, **94**, 175501 (2005). https://doi.org/10.1103/PhysRevLett.94.175501.

[18] Rosi NL, Eckert J, Eddaoudi M, Vodak DT, Kim J, O'keeffe M, Yaghi OM. Hydrogen storage in microporous metal-organic frameworks. Science, **300**, 1127 (2003). https://doi.org/10.1126/science.1083440.

[19] McKeown NB, Gahnem B, Msayib KJ, Budd PM, Tattershall CE, Mahmood K, Tan S, Book D, Langmi HW, Walton A. Towards polymer-based hydrogen storage materials: engineering ultramicroporous cavities within polymers of intrinsic microporosity. Angew Chem Int Ed, **45**, 1804 (2006). https://doi.org/10.1002/anie.200504241.

[20] Kim JD, Roh JS, Kim MS. Effect of carbonization temperature on crystalline structure and properties of isotropic pitch-based carbon fiber. Carbon Lett, **21**, 51 (2017). http://dx.doi.org/10.5714/CL.2017.21.051.

[21] Kim DK, An KH, Bang YH, Kwac LK, Oh SY, Kim BJ. Effects of electrochemical oxidation of carbon fibers on interfacial shear strength using a micro-bond method. Carbon Lett, **19**, 32 (2016). http://dx.doi.org/10.5714/CL.2016.19.032.

[22] Farooq U, Doh CH, Pervez SA, Kim DH, Lee SH, Saleem M, Sim SJ, Choi JH. Rate-capability response of graphite anode materials in advanced energy storage systems: a structural comparison. Carbon Lett, **17**, 39 (2016). http://dx.doi.org/10.5714/CL.2016.17.1.039.

[23] Lototskyy M, Yartys VA. Comparative analysis of the efficiencies of hydrogen storage systems utilising solid state H storage materials. J Alloys Compd, **645**, S365 (2015). https://doi.org/10.1016/j.jallcom.2014.12.107.

[24] Elias DC, Nair RR, Mohiuddin TMG, Morozov SV, Blake P, Halsall MP, Ferrari AC, Boukhvalov DW, Katsnelson MI, Geim AK, Novoselov KS. Control of graphene's properties by reversible hydrogenation: evidence for graphane. Science, **323**, 610 (2009). https://doi.org/10.1126/science.1167130.

[25] Yasmin A, Luo JJ, Daniel IM. Processing of expanded graphite reinforced polymer nanocomposites. Compos Sci Technol, **66**, 1182 (2006). https://doi.org/10.1016/j.compscitech.2005.10.014.

[26] Im JS, Kwon O, Kim YH, Park SJ, Lee YS. The effect of embedded vanadium catalyst on activated electrospun CFs for hydrogen storage. Microporous Mesoporous Mater, **115**, 514 (2008). https://doi.org/10.1016/j.micromeso.2008.02.027.

[27] Mu Y, Rabaey K, Rozendal RA, Yuan ZG, Keller J. Decolorization of azo dyes in bioelectrochemical systems. Environ Sci Technol, **43**, 5137 (2009). https://doi.org/10.1021/es900057f.

[28] Li ZQ, Lu CJ, Xia ZP, Zhou Y, Luo Z. X-ray diffraction patterns of graphite and turbostratic carbon. Carbon, **45**, 1686 (2007). https://doi.org/10.1016/j.carbon.2007.03.038.

[29] Kim BJ, Lee YS, Park SJ. A study on the hydrogen storage capacity of Ni-plated porous carbon nanofibers. Int J Hydrogen Energy, **33**, 4112 (2008). https://doi.org/10.1016/j.ijhydene.2008.05.077.

[30] Choi EK, Jeon IY, Oh SJ, Baek JB. "Direct" grafting of linear macromolecular "wedges" to the edge of pristine graphite to prepare edge-functionalized graphene-based polymer composites. J Mater Chem, **20**, 10936 (2010). https://doi.org/10.1039/C0JM01728K.

[31] Zhao H, Lin R. Preparation of boric acid modified expandable graphite and its influence on polyethylene combustion characteristics. J Chil Chem Soc, **61**, 2767 (2016). http://dx.doi.org/10.4067/S0717-97072016000100004.

[32] Kim BJ, Lee YS, Park SJ. Preparation of platinum-decorated porous graphite nanofibers, and their hydrogen storage behaviors. J Colloid Interface Sci, **318**, 530 (2008). https://doi.org/10.1016/j.jcis.2007.10.018.

[33] Lee HM, Heo YJ, An KH, Jung SC, Chung DC, Park SJ, Kim BJ. A study on optimal pore range for high pressure hydrogen storage behaviors by porous hard carbon materials prepared from a polymeric precursor. Int J Hydrogen Energy, **43**, 5894 (2018). https://doi.org/10.1016/j.ijhydene.2017.09.085.

[34] Bond WL. Precision lattice constant determination. Acta Crystallogr, **13**, 814 (1960). https://doi.org/10.1107/S0365110X60001941.

[35] Aga RS, Fu CL, Krčmar M, Morris JR. Theoretical investigation of the effect of graphite interlayer spacing on hydrogen absorption. Phys Rev B, **76**, 165404 (2007). https://doi.org/10.1103/PhysRevB.76.165404.

[36] Lin X, Telepeni I, Blake AJ, Dailly A, Brown CM, Simmons JM, Zoppi M, Walker GS, Thomas KM, Mays TJ, Hubberstey P, Champness NR, Schröder M. High capacity hydrogen adsorption in Cu(II) tetracarboxylate framework materials: the role of pore size, ligand functionalization, and exposed metal sites. J Am Chem Soc, **131**, 2159 (2009). https://doi.org/10.1021/ja806624j.

[37] Yuan S, Dorney B, White D, Kirklin S, Zapol P, Yu L, Liu DJ. Microporous polyphenylenes with tunable pore size for hydrogen storage. Chem Commun, **46**, 4547 (2010). https://doi.org/10.1039/C0CC00235F.

[38] Kim BJ, Lee YS, Park SJ. Novel porous carbons synthesized from polymeric precursors for hydrogen storage. Int J Hydrogen Energy, **33**, 2254 (2008). https://doi.org/10.1016/j.ijhydene.2008.02.019.